Aerosol and Air Quality Research, 18: 1531–1544, 2018

ISSN: 1680-8584 print / 2071-1409 online
doi: 10.4209/aaqr.2017.11.0500

Pollution Characteristics of Water-soluble Ions in Aerosols in the Urban Area in Beibei of Chongqing

Yanpei Li[1], Qingju Hao[1], Tianxue Wen[2], Dongsheng Ji[2], Zirui Liu[2], Yuesi Wang[2], Xiaoxi Li[1], Xinhua He[1], Changsheng Jiang[1*]

[1] *Key Laboratory of Eco-environments in Three Gorges Reservoir Region (Ministry of Education), College of Resources and Environment, Southwest University, Chongqing 400715, China*
[2] *State Key Laboratory of Atmospheric Boundary Layer Physics and Atmospheric Chemistry, Institute of Atmospheric Physics, Chinese Academy of Sciences, Beijing 100029, China*

ABSTRACT

To investigate the pollution characteristics of water-soluble ions in aerosols in the urban area of Beibei District, Chongqing, graded aerosol samples were continuously collected by a cascade impactor (Andersen) from March 2014 till February 2015. Water-soluble ions, namely, Na^+, NH_4^+, K^+, Mg^{2+}, Ca^{2+}, F^-, Cl^-, NO_3^- and SO_4^{2-} in different particle-size ranges (< 0.43, 0.43–0.65, 0.65–1.10, 1.10–2.10, 2.10–3.30, 3.30–4.70, 4.70–5.80, 5.80–9.00 and 9.00–100 μm), were measured by ion chromatography. The results showed that Mg^{2+}, Ca^{2+} and F^- mainly appeared in coarse particles, and other ions were mainly distributed in fine particles. SO_4^{2-} was mainly distributed in the droplet mode in spring and autumn from in-cloud processes, while SO_4^{2-} had both condensation and droplet modes in summer from the oxidation of SO_2. NH_4^+ and SO_4^{2-} were mainly present in the form of NH_4HSO_4 in aerosols. Except during summer, NO_3^- mostly existed in the forms of NH_4NO_3 in fine particles and $Ca(NO_3)_2$ in coarse particles. Na^+ was single-peaked in spring and summer and double-peaked in autumn and winter. Fine-mode K^+ showed a single-peak distribution in every season. The existent forms of Cl^- were KCl in the fine mode and $CaCl_2$ in the coarse mode. Mg^{2+} was mainly distributed in coarse particles, which showed a bimodal pattern distribution in spring and summer. Ca^{2+} mainly existed in coarse modes, whose concentrations increased with particle size. The emissions from motor vehicle exhaust, combustion processes, soil and construction dust were the major sources of water-soluble ions in this area. SOR (the sulfur oxidation ratio) was the highest in summer and the lowest in winter, but NOR (the nitrogen oxidation ratio) was highest in winter. The SOR values for condensation-mode (0.43–0.65 μm) exceeded 0.10 only in summer. SOR was considerably higher than NOR for the same particle sizes during the whole year.

***Keywords*:** Water-soluble ions; Fine mode; Coarse mode; Size distribution.

INTRODUCTION

Atmospheric aerosols, also known as atmospheric particles, refer to a general designation of solid and liquid particles suspended in the atmosphere and usually distributed in particle sizes of 0.001–100 μm (Yang *et al.*, 2012). The chemical composition of aerosols is complex, and they are from numerous sources. The aerosols contain many toxic and harmful substances prone to various physical and chemical reactions in the air (Su *et al.*, 2018). Previous studies have shown that aerosols have effects on particle growth, gas-to-particle conversion, removal mechanisms, solar radiation, visibility and the formation of cloud condensation nuclei, mainly depending on their particle size and chemical composition (Henning *et al.*, 2003; Zhou *et al.*, 2010). In the environment, the most important aerosol processes occur with the following size modes: Aitken (< 0.1 μm), condensation (~0.1–0.5 μm), droplet (~0.5–2.0 μm), and coarse (> 2.0 μm) (Seinfeld and Pandis, 2006). The droplet-mode particles are produced by in-cloud processing or aqueous reactions (Chen *et al.*, 2016), whereas the coarse-mode aerosols are typically derived from different sources.

Water-soluble ions, as the important components of aerosols, are mainly composed of sulfates, nitrates, ammonium salts and other substances (Wang *et al.*, 2005a). They can change the size, quantity, composition and life of the aerosol by self hygroscopicity and affect the particle size distribution and the formation of cloud condensation

* Corresponding author.
E-mail address: jiangcs@126.com

nuclei (Yue *et al.*, 2016). Meanwhile, nitrate and sulfate are the most important light extinction components; an increase in their concentrations can significantly reduce the visibility (Chen *et al.*, 2003; Chen *et al.*, 2014). Cl^-, SO_4^{2-}, NO_3^- and other soluble anions are the main acidic ions in the atmosphere (Kerminen *et al.*, 2011); their concentration can directly affect the acidity of atmospheric precipitation and therefore the global climate and terrestrial environment. Moreover, water-soluble ions can combine with carbonaceous aerosols to form aerosol particles with different mixing states, greatly changing the radiation function of aerosols, and then cause haze and other extreme weather (Chen *et al.*, 2010; Szopa *et al.*, 2013). Water-soluble ions are also easily dissolved in rain and can migrate with rainfall in the terrestrial environment (Shen *et al.*, 2012). Last but not least, water-soluble ions can have synergistic effects (such as PAHS and arsenic), resulting in increased solubility of these substances, which results in greater harm to human health (Chueinta *et al.*, 2000).

At present, the analysis of the pollution characteristics of water-soluble ions in aerosols has become a hot topic around the world (Wang *et al.*, 2001; Wang *et al.*, 2015; Cao *et al.*, 2016; Begam *et al.*, 2017; He *et al.*, 2017). Chongqing is an industrial megacity in southwest China and one of the important industrial bases in China. It is known as a "fog capital", in which air pollution is quite serious. In recent years, numerous studies on the pollution of water-soluble ions in aerosols in Chongqing have been reported. For example, Jiang *et al.* (2009) studied the background pollution characteristics of 9 kinds of water-soluble ions in PM_{10} in the main urban area of Chongqing and Jinyun Mountain. He *et al.* (2012) analyzed the seasonal variations of 8 kinds of water-soluble ions in $PM_{2.5}$ at both urban and rural sites of Beijing and Chongqing to explore their relationship with acidity. Tian *et al.* (2016a) analyzed 5 kinds of cations and 6 kinds of anions in $PM_{2.5}$ in Yubei District of Chongqing. Determination of the size distributions of water-soluble ions in aerosols can help understand the transformation, transport and fate of aerosols, though only a few studies have focused on their particle size distributions in Chongqing. Moreover, most of the previous studies in Chongqing have focused only on measurements in each season, and distinctive seasonal variations due to different meteorological and anthropogenic activities have rarely been discussed. Therefore, this study analyzed the concentration variations, particle size distributions and influencing factors of 9 kinds of water-soluble ions over four seasons from March 2014 till February 2015 based on the monitoring data of water soluble ions in aerosols in Beibei District in Chongqing. The generated results reveal the sources, formation and transformation of particulate pollutants, and their environmental effects so as to provide more practical guidelines for better air pollution control in the tested region.

METHOD AND MATERICALS

Site Location and Sampling Method

The sampling site (29°48′43″N, 106°24′58″E) was located on the rooftop (282 m above the sea level) of the College of Resources and Environment building (35 m above ground) on the campus of Southwest University in the Beibei urban area in Chongqing, China (Fig. 1). The Beibei urban area is surrounded by Zhongliang Mountain (1000 m a.s.l. at the peak) to the south and Jinyun Mountain (951 m a.s.l. in the peak) to the north. The local air circulation in the sampling site is a little affected by the close educational and residential buildings with some small ups and downs. The site, representing a typical urban environment in the

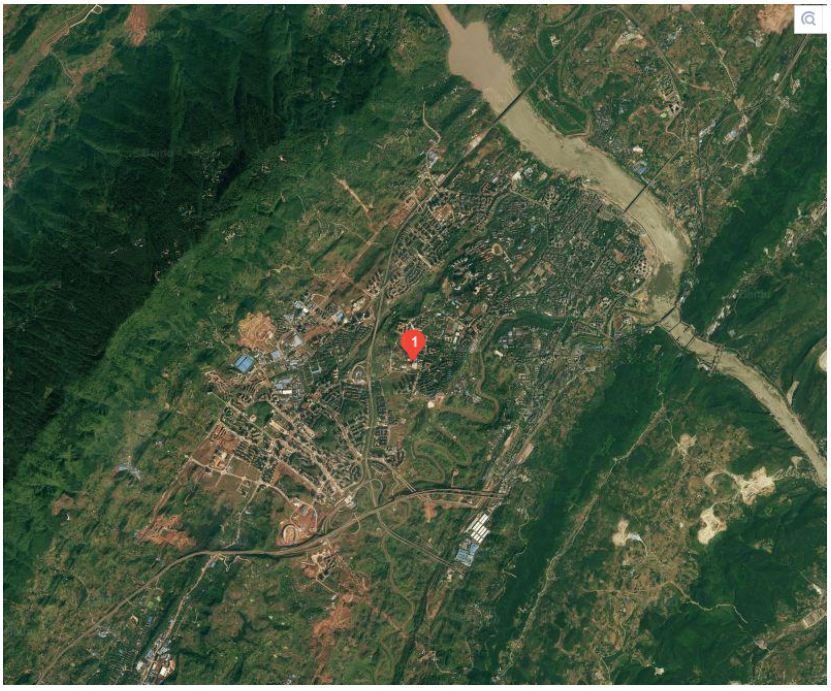

Fig. 1. A sky view of sampling site in the urban area of Beibei (29°48′43″N, 106°24′58″E), Chongqing, China.

Beibei District of the city of Chongqing, is about 30 m from a main city traffic road and about 800 m from the southbound intersection of a highway and has no direct industrial pollution sources within a 5 km distance.

Sampling Methods

The aerosol particles were collected by an Andersen Impact Grading Sampler (Andersen, Series 20-800, USA) according to the following size ranges: < 0.43, 0.43–0.65, 0.65–1.1, 1.1–2.1, 2.1–3.3, 3.3–4.7, 4.7–5.8, 5.8–9.0 and 9.0–100 μm. The sampling flow rate was 28.30 L min^{-1}, and the sampling filters were polyester fibre films (Thermoelectric, USA). A 48-hour continuous air sampling was taken once a week from March 2014 till February 2015 (from 11 a.m. LST on the first day to 11 a.m. LST on the third day). During the experiment, a total of 396 filters from 44 valid sampling groups were obtained and stored in refrigerators at –18°C for further analyses.

Sampling Analyses

A total of 30.00 mL of deionized water (18.20 MΩ·cm) were firstly added to a plastic bottle containing a sampled filter, and then the water-soluble components in the sample were extracted by ultrasonic wave for 30 min. After the water extracts were filtered by a 0.45-μm membrane (Membrana, Micro PES, Germany), the concentrations of cations (Na^+, NH_4^+, K^+, Mg^{2+}, Ca^{2+}) and anions (F^-, Cl^-, NO_3^-, SO_4^{2-}) in the filtrate were determined by an ICS-90 ion chromatography system (Dionex, USA). The conditions for the cation detection were: CS12A column, CSRS II suppressor; Eluent: 22.00 mmol L^{-1} MSA; and flow-rate: 1.00 mL min^{-1}. The conditions for the anion detection were: Dionex AS14A separation column, AMMS III suppressor; Eluent: 1.00 mmol L^{-1} $NaHCO_3$, 3.50 mmol L^{-1} Na_2CO_3; and flow rate: 1.00 mL min^{-1}. The detection limits of Na^+, NH_4^+, K^+, Mg^{2+}, Ca^{2+}, F^-, Cl^-, NO_3^- and SO_4^{2-} were 0.001, 0.001, 0.002, 0.001, 0.003, 0.001, 0.002, 0.005 and 0.004 mg L^{-1}, respectively.

Date Analyses

The size distributions of these 9 water-soluble ions in each season were plotted by Origin 9.1 software. Statistical analyses (correlation and principal component analyses) were performed with an SPSS 17.0. Correlation analyses of water-soluble ions in the $PM_{2.1}$ and $PM_{9.0}$ used Pearson correlation coefficients so that they could reveal the binding modes and the origin of these ions in the aerosol could be inferred. In order to better explore the main sources of water-soluble ions in the aerosols in Beibei District, the principal component analysis (PCA) was used to classify and analyze these 9 water-soluble ions in the $PM_{2.1}$ and $PM_{9.0}$.

Quality Assurance and Quality Control (QA/QC)

All samples were collected on quartz fiber filters (81 mm in diameter) during the study period. The quartz fiber filters were pre-fired (2 h at 800°C) to remove all organic material and weighed before and after sampling using a microbalance with a sensitivity of ± 0.01 mg. The filters were conditioned in a dryer at 25 ± 3°C under a RH (relative humidity) of 22 ± 3% for 72 h before each weighing. After reweighing, the sampling filters were immediately stored in a freezer at –20°C to avoid the loss of semi-volatiles. The samplers were cleaned using an ultrasonic bath before sampling. In addition, the sampling flow rates were calibrated before each sampling and monitored using a flow meter during each sampling. One group of blank quartz filters was used to determine background contamination. The ions were quantified by external standard curves every week, and one trace calibration standard solution was used to check the curve each day. The limit of detection was less than 0.02 μg m^{-3} for all ions when the injection volume was 100 μL (Tian *et al.*, 2016b; Wang *et al.*, 2017).

RESULTS AND DISSUSSION

The Particle Size Distributions of Water-Soluble Ions in Spring

The Size Distribution of Primary Ions

To analyze the contents of each water-soluble ion, the collected aerosols were divided into two sizes as the coarse (> 2.10 μm) and fine (< 2.10 μm) particles. In terms of the aerodynamic diameter, the particle size distributions of various water-soluble ions in spring are shown in Figs. 2(a)–2(d). Table 1 shows the meteorological factors and SO_2 concentrations over four seasons from March 2014 till February 2015.

As shown in Fig. 2, the particle size distributions of 9 kinds of ions showed the following patterns: SO_4^{2-}, NH_4^+, NO_3^-, Cl^-, Na^+ and K^+ were mainly distributed in the fine particles, whereas Mg^{2+}, Ca^{2+} and F^- were mainly present in the coarse particles.

Fig. 2(a) shows that the peak of Na^+ concentration was at 1.10–2.10 μm, but Na^+ was roughly equivalent in the coarse and fine particles. The fine mode Na^+ was mainly from the anthropogenic source, while the coarse mode Na^+ was mainly from the wind-drifting sand and sea salt (Tao *et al.*, 2014). Chongqing is located in an inland region with few marine sources, and mainly fueled by fossil fuels, so Na^+ in the coarse particles probably came from dust from non-marine sources.

The distribution of K^+ showed a single peak, and the peak mainly appeared in the 0.43–1.10 μm particle size, which was roughly the same as the distribution of K^+ in Beijing (Yang *et al.*, 2015). The K^+ in the fine particles was mainly from biomass burning, while in the coarse particles, it was mainly from soil and marine salts (Parmar *et al.*, 2001; Sorooshian *et al.*, 2013). A unique mountainous terrain, which is dominated by low mountains, away from the ocean, the mountain core by the Triassic Jialing River limestone composition, emerged "one mountain, one trough, two ridge", and frequent agricultural activities (the self-sufficient agriculture of rice, corn and wheat planting) in Beibei District, most likely, were the important reasons that K^+ was mainly distributed in the fine particles below 1.10 μm.

Mg^{2+} showed a bimodal distribution, and the peak appeared at size ranges of 2.10–3.30 μm and 5.80–9.00 μm,

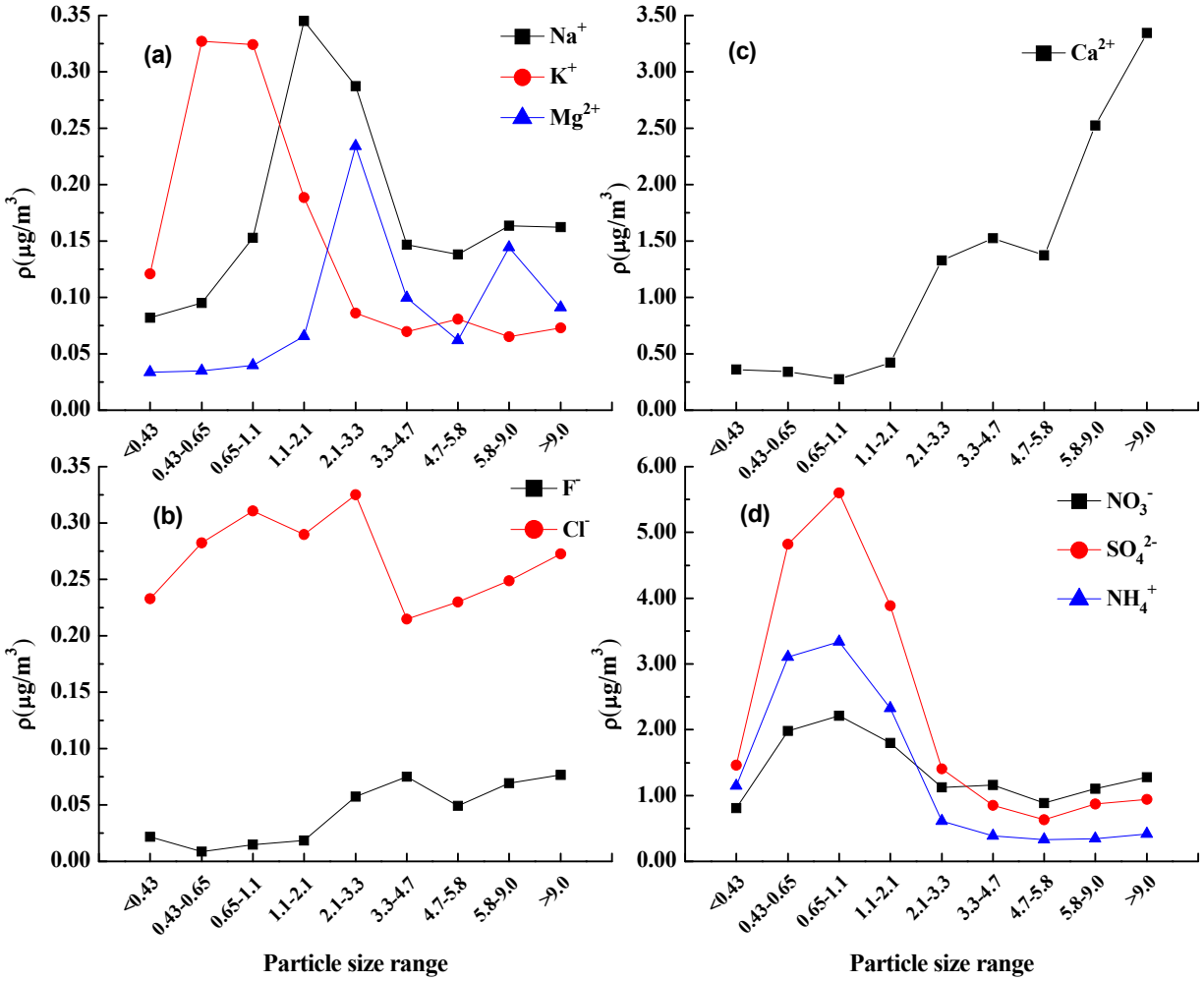

Fig. 2. Size distributions of water-soluble ions in the aerosol in spring in the urban area of Beibei.

Table 1. The meteorological parameters and atmospheric pollutants during four seasons.

Parameter	Spring	Summer	Autumn	Winter
Sunshine hours (h)	126	326.7	121.1	64.2
Ly Wind speed (m s^{-1})	13.77	13.57	12.09	12.70
Air temperature (°C)	18.47	27.16	19.70	10.24
Relative humidity (%)	77.98	75.66	82.97	78.31
Precipitation (mm)	418.2	598.7	394.9	49.5
SO_2 (μg m^{-3})	28.5	15.1	16.3	34.4
NO_2 (μg m^{-3})	36.5	31.5	39.0	40.8
O_3 (μg m^{-3})	37.1	58.8	26.9	15.6

respectively. The mass concentration of Ca^{2+} increased with the particle size, and the maximum concentration appeared at 9.0 μm (3.34 μg m^{-3}). The coarse mode size distributions of Mg^{2+} and Ca^{2+} were commonly observed in urban environments (Tao *et al.*, 2014; Yang *et al.*, 2015) and were mostly from natural sources, such as the lifting of dust or mechanical abrasion processes. The main reason for the distribution characteristics of Ca^{2+} in particles in Beibei District might be the continuous urbanization in recent years and the extensive use of cement, lime and other building materials, resulting in the increase of Ca^{2+} in coarse particles. These results were similar to the concentration peak values of Mg^{2+} and Ca^{2+} in Lhasa, China (Wan *et al.*, 2016).

F^- appeared as a single-peak distribution and was mainly distributed in coarse particles, with a peak in the range of 3.30–4.70 μm. The concentration of F^- was relatively low, so there was no more analysis here.

Cl^- showed a double distribution, with peaks in the ranges of 0.65–1.10 μm and 2.10–3.30 μm. The coarse mode Cl^-, like Na^+, was mainly from the sea salt; the fine mode Cl^- was mainly derived from power plants, incinerators and other combustion processes, motor vehicle exhaust and other artificial sources. Although there were few marine

sources, Cl^- correlated well with Ca^{2+} with a correlation coefficient of 0.88 in the range of 2.10–3.30 μm. Generally, Cl^- mostly combined with Ca^{2+} to form $CaCl_2$ in the coarse particles.

The Size Distribution of Secondary Ions

The particle size distributions of SNA (SO_4^{2-}, NH_4^+ and NO_3^-) were roughly the same; all showed a unimodal distribution, with peaks between 0.65 and 1.10 μm (Fig. 2(d)). These results indicated that the relationships of these three ions, which were the main components of fine particles, were close. This was quite different from the size distribution characteristics of SNA in the Jing-Jin-Ji urban region, which had a bimodal size distribution with the fine mode ranging 0.43–1.1 μm and the coarse mode, 4.70–5.80 μm (Li *et al.*, 2013).

SO_4^{2-} was mainly distributed in the droplet mode, which was attributed to the in-cloud processes (John *et al.*, 1990) because the growth of condensation mode particles by the accretion of water vapor or by the gas phase and/or aqueous aerosol phase of sulfate production could not explain the existence of the droplet mode. In this study, the SO_2 concentrations were 28.5 μg m^{-3} in spring (Table 1). The mole ratio of sulfate in the range of 0.65–1.10 μm to SO_2 was about 0.13, and higher precipitation (418.20 mm) and relative humidity (RH > 75%) in spring indicate that the in-cloud formation of sulfate might be important in sulfate formation.

NH_4^+ was mainly distributed in the fine particles, which indicated that it mainly came from NH_3 released by anthropogenic sources such as agriculture, industry and aquaculture (Wan *et al.*, 2016). NH_3 mainly reacts with acid gases such as H_2SO_4, HNO_3 and HCl to produce $(NH_4)_2SO_4$, NH_4HSO_4, NH_4NO_3 and NH_4Cl. Based on the correlation between NH_4^+ and SO_4^{2-} being the best (r = 0.99) and the ratio of $[NH_4^+]/[SO_4^{2-}]$ in the fine particles being 0.63 (< 1.0), NH_4HSO_4 was the major form of ammonium in $PM_{2.1}$.

The mode distributions of nitrate are governed by the thermodynamic equilibrium of $HNO_3(g) + NH_3(g) \rightleftharpoons NH_4NO_3$ (s, aq), which is affected by the RH, temperature and the concentrations of $(NH_4)_2SO_4$, $HNO_3(g)$ and $NH_3(g)$ (John *et al.*, 1990). When the thermodynamic equilibrium favors the formation of NH_4NO_3 (s, aq), nitrate will dominate in the fine mode. On the other hand, if the formation of NH_4NO_3 (s, aq) is not favored, the reactions of HNO_3 with $CaCO_3$ or NaCl in the coarse mode become important (Pakkanen *et al.*, 1996; Zhuang *et al.*, 1999). Due to the concentration of NO_3^- mainly distributed in the fine particles, and the air temperature was lower (18.47°C), which can infer NO_3^- in spring in Beibei District existed mainly in the form of NH_4NO_3.

The Particle Size Distributions of Water-Soluble Ions in Summer

The Size Distribution of Primary Ions

The particle size distributions of various water-soluble ions in summer, in terms of the aerodynamic diameter, are shown in Figs. 3(a)–3(d).

Na^+ held a single-peak distribution, mainly distributed as fine particles, with a peak in the range of 0.65–1.10 μm, which mainly came from the anthropogenic sources. The concentration of Na^+ was substantially decreased compared with in spring.

The distribution of K^+ also showed a single-peak, and the peak mainly appeared in the particle size range of 0.43–0.65 μm, which was approximately similar to that in spring.

Mg^{2+} showed a bimodal distribution, and the peaks appeared in the ranges 2.10–4.70 μm and > 5.80 μm, respectively. The mass concentration of Ca^{2+} was the same as it was in spring. The F^- concentration was very low for each particle size. Cl^- showed a double distribution, with peaks in the ranges 0.43–1.10 μm and 4.70–5.80 μm, and the second peak was far larger than the first peak. The proportion of Mg^{2+} in coarse particles was also increased; thus the coarse mode Cl^- might have existed in the form of $CaCl_2$ or $MgCl_2$ (Fig. 3).

The Size Distribution of Secondary Ions

In summer, the MMAD (mass median aerodynamic diameter) of SO_4^{2-} in the fine mode appeared in the range of 0.43–0.65 μm, which was decreased to a grain level when compared with that in spring. Although the precipitation was largest in summer compared with the other three seasons (Table 1), the highest average temperature (27.16°C) and the most sunshine hours (326.7 h) favored the transformation of SO_2 into SO_4^{2-} by homogeneous reactions. So the accumulation mode of SO_4^{2-} in the range of 0.43–0.65 μm was mainly from the oxidation of SO_2 with subsequent hygroscopic growth (Wang *et al.*, 2005a). But since the rate of in-cloud oxidation of SO_2 could reach 100% per hour (Meng and Seinfeld, 1994), the mole ratio of sulfate in the range of 0.43–0.65 μm to SO_2 was about 0.20, and part of the fine mode of SO_4^{2-} may also have originated in in-cloud processes. Thus, SO_4^{2-} was distributed in both the condensation mode and droplet mode in summer.

The NH_4^+ size distributions were roughly the same as SO_4^{2-}, with peaks all in the range of 0.43–0.65 μm, which indicated that the relationship of the two ions was close. NH_4^+ and SO_4^{2-} in summer were in great agreement with the relative humidity in the atmosphere (r > 0.80). This is because the higher relative humidity is beneficial to the transformation of NH_3 and SO_2 to ammonium salts and sulfate (Dlugi *et al.*, 1981). SO_4^{2-} mostly combined with NH_4^+ to form $(NH_4)_2SO_4$ or NH_4HSO_4. The mole ratio of NH_4^+ to SO_4^{2-} in the fine particles was 0.52 (< 1.0), so it mainly existed in the form of NH_4HSO_4.

Nitrates showed a double distribution, with peaks in the ranges of 0.43–0.65 μm and > 9.00 μm, and the concentrations were roughly the same between the fine and coarse modes. The fine mode NO_3^- mainly existed in the form of NH_4NO_3 in the atmosphere, which had an obviously negative correlation with air temperature ($P < 0.01$). NH_4NO_3 had little thermal stability; it could be decomposed easily by high air temperature (27.16°C) in summer and release gases such as NH_3 and NO_x, resulting in a reduction in NH_4^+ and NO_3^- concentrations in fine particles (Li *et al.*, 2017). The coarse-grained NO_3^- was the result of a combination of precursors that might have come from vehicle exhaust, high

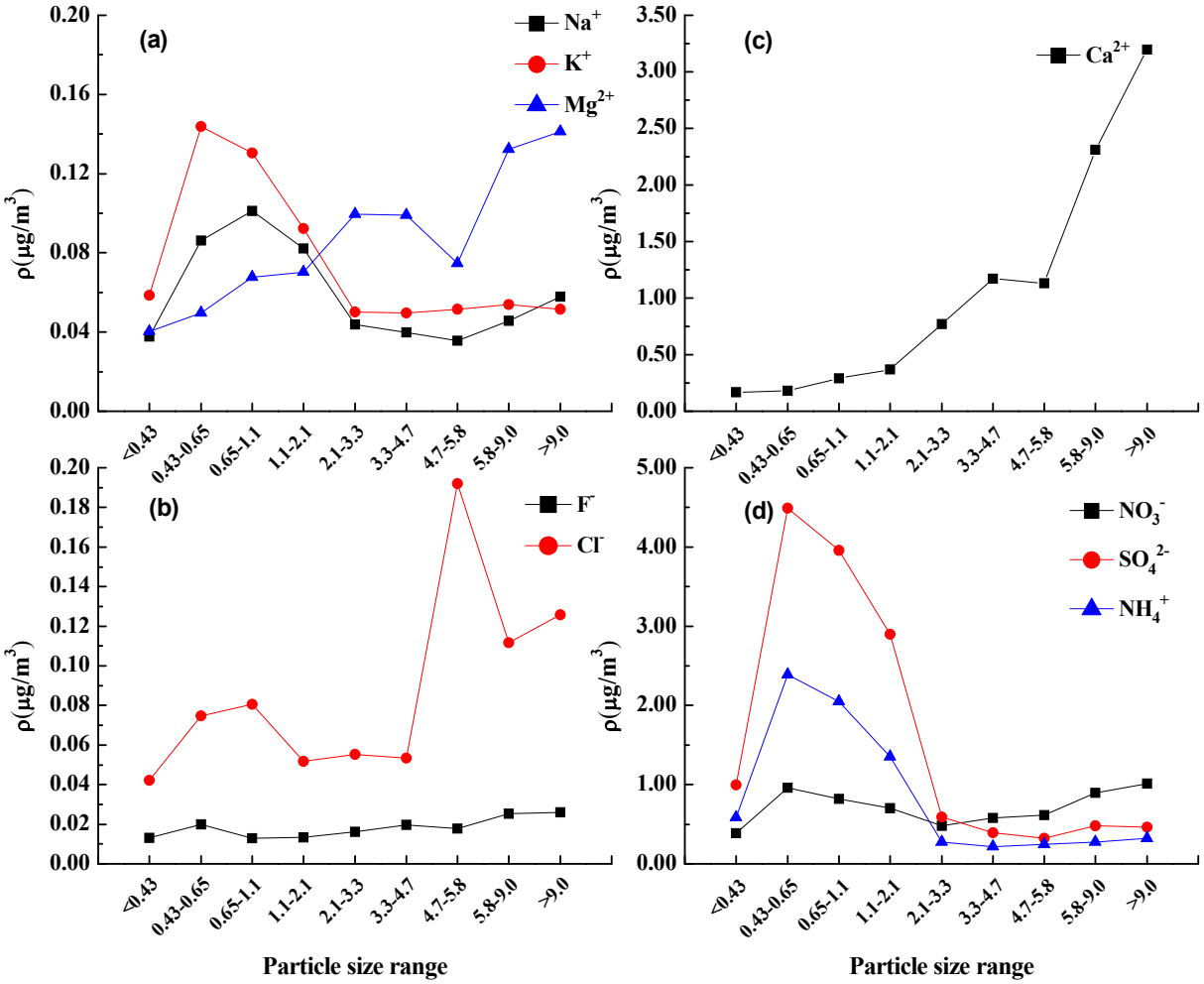

Fig. 3. Size distributions of water-soluble ions in the aerosol in summer in the urban area of Beibei.

temperature combustion and crustal material, such as Ca^{2+} and Mg^{2+}, or sea salts, such as Na^{+} and K^{+} (Imhof *et al.*, 2006). Due to few marine sources, a higher correlation with Ca^{2+} (r = 0.98), and the highest concentration (Ca^{2+}), NO_3^{-} in the coarse mode existed mainly in the form of $Ca(NO_3)_2$.

The Particle Size Distributions of Water-Soluble Ions in Autumn

The Size Distribution of Primary Ions

The particle size distributions of various water-soluble ions in autumn, in terms of the aerodynamic diameter, are shown in Figs. 4(a)–4(d).

Na^{+} appeared to have double peaks, and the peak concentrations appeared in the ranges of 1.10–2.10 μm and 5.80–9.00 μm. This was similar to the distribution of Na^{+} in the Beijing region (Yang *et al.*, 2015), but the particle size ranges of the two peaks that appeared in the coarse and fine particles were a little different.

K^{+} was a single-peak distribution, mainly distributed in fine particles, with a peak in the range of 0.65–2.10 μm; the source was the same as in spring. The F^{-} concentration was still low in each particle size range, mainly existing in the coarse particles.

Cl^{-} showed a double distribution, with peaks in the ranges of 0.65–1.10 μm and 3.30–4.70 μm, and the first peak was larger than the second peak. Cl^{-} mainly existed in fine particles, indicating that it was mainly derived from power plants, incinerators and other combustion processes, motor vehicle exhaust and other artificial sources in summer, which was the same as distribution characteristics of Cl^{-} in Beijing (Yang *et al.*, 2015).

Mg^{2+} and Ca^{2+} still mainly existed in coarse particles; the concentration increased with particle size but was obviously lower than in other seasons. The reasons may be as follows: The average precipitation in autumn of 2014 in Chongqing was twice that of previous years, the sunshine hours were fewer, and the relative humidity was higher (RH = 82.97%), the wet deposition process has a certain scavenging effect on the dust in the air through it. Besides, the wind speed (1.21 m s^{-1}) in autumn was low, which was not conducive to the diffusion of dust into the air; these may be the main reasons that the concentrations of Mg^{2+} and Ca^{2+} were lower in autumn but higher in other seasons.

The Size Distribution of Secondary Ions

Fig. 4(d) shows particle size distributions of SNA (SO_4^{2-}, NH_4^{+} and NO_3^{-}); all appear to be single-peak distributions, but peaks were not exactly the same.

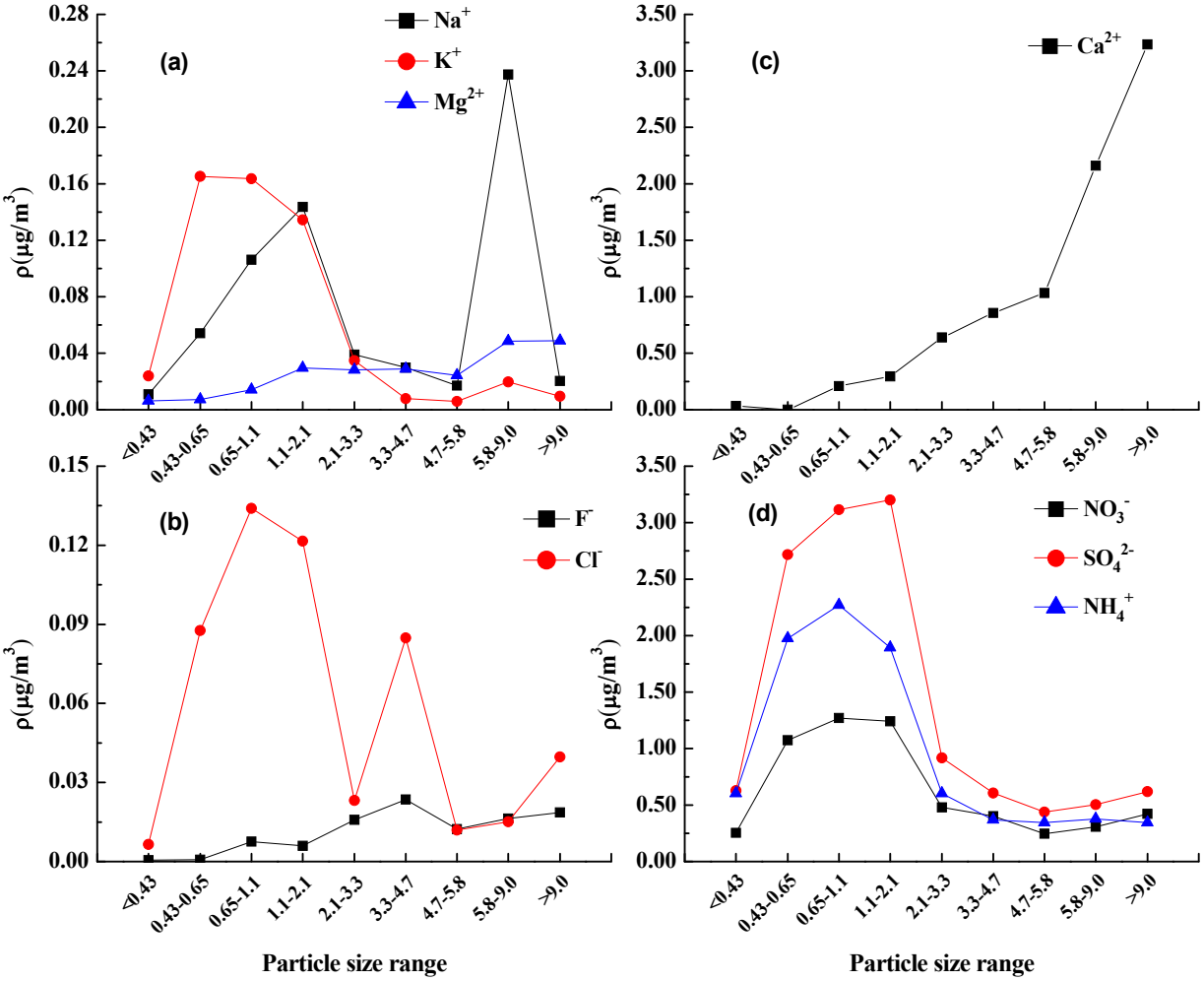

Fig. 4. Size distributions of water-soluble ions in the aerosol in autumn in the urban area of Beibei.

SO_4^{2-} was mainly distributed in the droplet mode with a peak in the range of 0.65–2.10 μm, elevated a grain level when compared with that in summer. As shown in Table 1, the mole ratio of sulfate in the range of 0.65–2.10 μm to SO_2 was about 0.26, the highest relative humidity (RH = 82.97%) and fewer sunshine hours in autumn (121.1), indicating that in-cloud formation of sulfate may be important in sulfate formation.

NH_4^+ and NO_3^- mainly existed in the range of 0.65–1.10 μm in the droplet mode; their correlation was great (r = 0.81). NH_4^+ and NO_3^- in the fine mode mainly existed in the form of NH_4NO_3, which was similar to that in spring and summer.

The Particle Size Distributions of Water-Soluble Ions in Winter

The Size Distribution of Primary Ions

The particle size distributions of various water-soluble ions in autumn, in terms of the aerodynamic diameter, are shown in Figs. 5(a)–5(d).

Fig. 5 shows particle size distributions of K^+ and Cl^- being almost same: Both were a single-peak distribution, with the peak in the range of 0.65–1.10 μm, indicating that the relationship of the two ions is close (r = 0.80). During the Spring Festival in Chongqing, due to the firecrackers, fireworks and biomass burning, a large amount of chlorine was generated and entered the aerosol. At that moment, Cl^- mainly combined with K^+ in the form of KCl.

Na^+ was a double peak type, and the peak concentrations appeared in the particle size ranges of 0.65–1.10 μm and 5.80–9.00 μm. The Ca^{2+} peak value of the coarse mode in winter was higher than in other seasons, indicating that there were more crustal sources in that season (Liu *et al.*, 2017). The concentrations of Mg^{2+} and F^- were low in each particle size, and the principal amounts appeared in the coarse mode.

The Size Distribution of Secondary Ions

Fig. 5 shows the particle size distributions of SNA (SO_4^{2-}, NO_3^- and NH_4^+) being almost the same: a unimodal distribution, with peaks all in the range of 0.65–1.10 μm, indicating that the relationships of these three ions are close (R_{SA} = 0.96, R_{NA} = 0.92, R_{SN} = 0.84).

SO_4^{2-} was mainly distributed in the droplet mode. Due to the fact that the precipitation was only 49.5 mm in winter and the sunshine hours were also fewer, SO_4^{2-} could be attributed to non-precipitation reactions in cloud droplets or droplets. Because the average temperature was very low compared with other seasons, NH_4^+ and NO_3^- in the fine

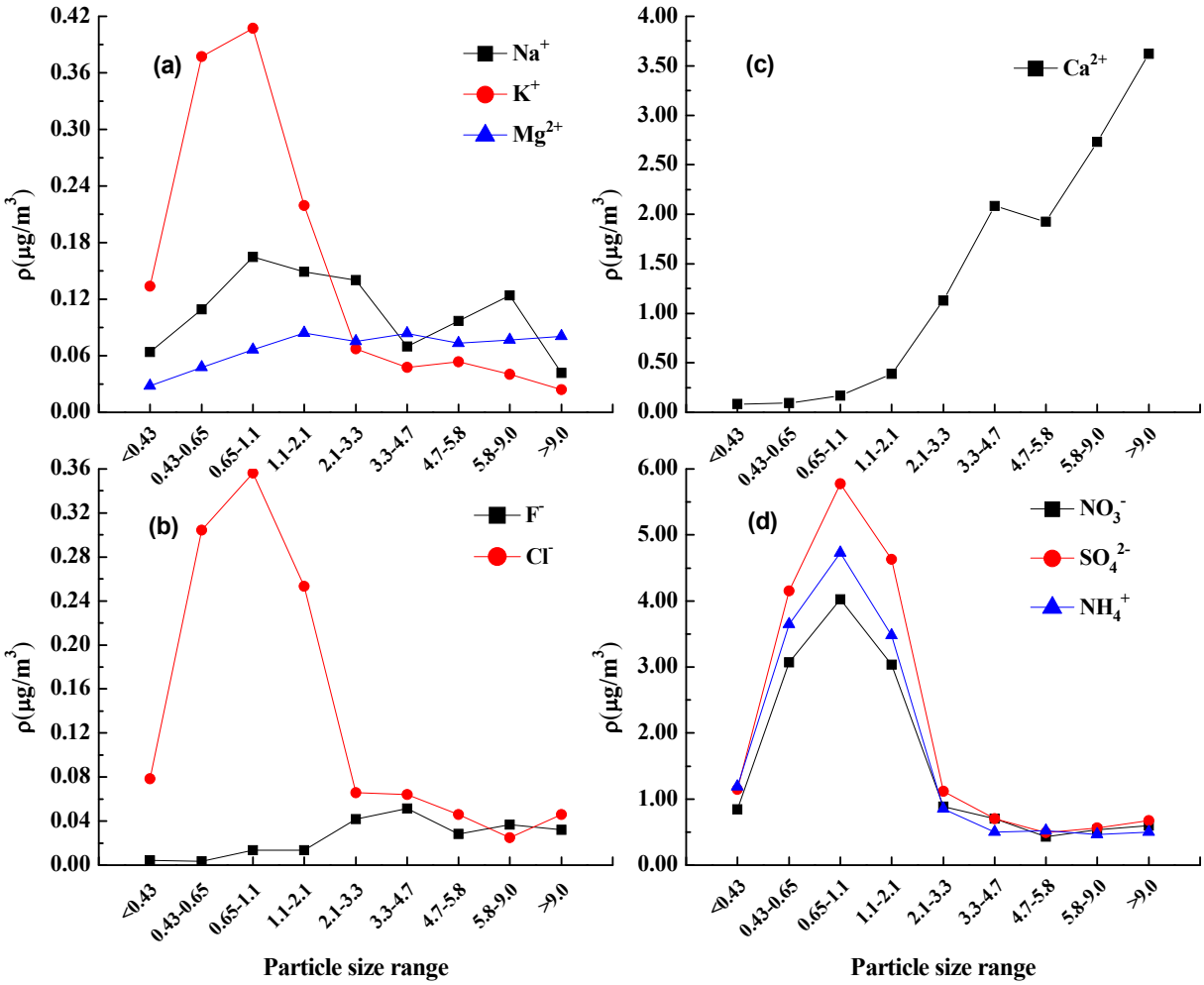

Fig. 5. Size distributions of water-soluble ions in the aerosol in winter in the urban area of Beibei.

mode mainly existed in the form of NH_4NO_3, which was similar to spring. In addition, $\rho(NO_3^-)$ in winter was significantly higher than other seasons in Fig. 5, which may be due to the fact that the particulate NO_3^- was mainly composed of volatile components and susceptible to winter temperatures, so relatively low temperatures and higher NO_x emissions were beneficial to the formation of NO_3^- in aerosols (Zhang *et al.*, 2011). At the same time, the atmospheric structure of the Beibei urban area was more stable in winter, and the inversion temperature was significant, which contributed to the transformation of SNA and led to higher concentrations in winter.

Balance and Correlation of Ions

The acidity-alkalinity of atmospheric aerosols has an important effect on the pH of precipitation, which may cause precipitation acidification or the acidity of precipitation to play a neutralizing role (Tang *et al.*, 2005). Some studies showed that NO_3^-, SO_4^{2-}, F^- and Cl^- are favorable for the acidity of aerosol, whereas NH_4^+, K^+, Na^+, Mg^{2+} and Ca^{2+} increase the pH of aerosol (Xu *et al.*, 2012). The ion balance is a good indicator in studying the acidity of aerosol, which is determined by both anion equivalents (AE) and cation equivalents (CE) calculated with the following equations:

AE (Anion equivalent) =

$$\frac{\rho(F^-)}{19}+\frac{\rho(Cl^-)}{35.5}+\frac{\rho(NO_3^-)}{62}+\frac{\rho(SO_4^{2-})}{48} \quad (1)$$

CE (Cation equivalent) =

$$\frac{\rho(Na^+)}{23}+\frac{\rho(NH_4^+)}{18}+\frac{\rho(K^+)}{39}+\frac{\rho(Mg^{2+})}{12}+\frac{\rho(Ca^{2+})}{20} \quad (2)$$

On the one hand, the correlation analysis between ions can reveal the binding modes of ions in aerosol; on the other hand, it can be used to infer the origin of the material. In this paper, the correlations among nine kinds of water-soluble ions in $PM_{2.1}$ and $PM_{9.0}$ were compared. The correlation coefficients between different ions are summarized in Tables 2 and 3.

As Tables 2 and 3 show, the correlations between the anions and cations were significant, indicating that the measured data was valid. The ratio of AE/CE in $PM_{2.1}$ was 0.67, while the ratio of $PM_{9.0}$ was 0.49, and the total cation concentration was distinctly higher than that of anion, namely, the anions from the aerosol in this area were relatively

Table 2. Correlation coefficients matrix for the concentrations of water-soluble ions in $PM_{2.1}$.

	Na^+	NH_4^+	K^+	Mg^{2+}	Ca^{2+}	F^-	Cl^-	NO_3^-	SO_4^{2-}	Σ(+)	Σ(–)
Na^+	1.00	0.37*	0.14	0.10	0.18	0.21	0.35*	0.35*	0.53**	0.44**	0.51**
NH_4^+		1.00	0.64**	0.13	0.06	0.22	0.76**	0.91**	0.82**	0.99**	0.94**
K^+			1.00	0.18	0.23	0.19	0.54**	0.71**	0.51**	0.68**	0.65**
Mg^{2+}				1.00	0.41**	0.25	0.07	0.24	0.23	0.21	0.25
Ca^{2+}					1.00	0.28	0.21	0.05	0.21	0.18	0.17
F^-						1.00	0.21	0.15	0.39**	0.27	0.34*
Cl^-							1.00	0.70**	0.49**	0.78**	0.68**
NO_3^-								1.00	0.66**	0.91**	0.87**
SO_4^{2-}									1.00	0.84**	0.94**
Σ(+)										1.00	0.96**
Σ(–)											1.00

Note: * represents significant correlation ($P < 0.05$), ** represents highly significant correlation ($P < 0.01$).

Table 3. Correlation coefficients matrix for the concentrations of water-soluble ions in $PM_{9.0}$.

	Na^+	NH_4^+	K^+	Mg^{2+}	Ca^{2+}	F^-	Cl^-	NO_3^-	SO_4^{2-}	Σ(+)	Σ(–)
Na^+	1.00	0.20	0.02	0.13	0.04	0.10	0.22	0.24	0.38*	0.28	0.34*
NH_4^+		1.00	0.57**	0.08	0.26	0.52**	0.57**	0.89**	0.79**	0.87**	0.89**
K^+			1.00	0.11	0.32*	0.55**	0.43**	0.68**	0.50**	0.59**	0.63**
Mg^{2+}				1.00	0.47**	0.19	0.50**	0.16	0.17	0.37*	0.24
Ca^{2+}					1.00	0.49**	0.31*	0.37*	0.39**	0.68**	0.43**
F^-						1.00	0.67**	0.55**	0.53**	0.63**	0.64**
Cl^-							1.00	0.57**	0.46**	0.62**	0.64**
NO_3^-								1.00	0.75**	0.86**	0.91**
SO_4^{2-}									1.00	0.81**	0.94**
Σ(+)										1.00	0.90**
Σ(–)											1.00

Note: * represents significant correlation ($P < 0.05$), ** represents highly significant correlation ($P < 0.01$).

depleted. This finding markedly differed from the results in the Jinyun Mountain area from January 2005 till May 2006 (He *et al.*, 2012), where the total anion concentration in TSP was higher than the cation concentration. These differences were large because of the significant increase in Ca^{2+} concentration caused by growing urban construction and road dust; it may also be the excessive NH_4^+, compared with previous years (Jiang *et al.*, 2009; He *et al.*, 2012), especially the existence of alkaline NH_4^+ (Satsangi *et al.*, 2013).

The correlation between SNA was significant in both $PM_{2.1}$ and $PM_{9.0}$ ($r \geq 0.75$), indicating that they may have the same secondary transformation source. Meanwhile, the correlation between the two secondary ions, NH_4^+ and NO_3^-, in $PM_{2.1}$ was far more significant, suggesting that they mainly existed in the form of NH_4NO_3 in the fine particles. Ca^{2+} and Mg^{2+} had a significant correlation in $PM_{2.1}$ but were poorly related to other ions, which indicated that Ca^{2+} and Mg^{2+} may have the same source. The result of Na^+ varied greatly among different particles: Na^+ showed a significant correlation with Cl^-, NO_3^- and SO_4^{2-} in $PM_{2.1}$ but was only significantly related to SO_4^{2-} in $PM_{9.0}$ ($P < 0.05$), indicating that Na^+ in the fine particles may exist in various forms such as NaCl, $NaNO_3$ and Na_2SO_4. However, in the coarse particles, the sodium salt was mainly in the form of Na_2SO_4. Cl^- had a low correlation with Na^+ in $PM_{9.0}$ but had strong correlation with other ions, indicating that the sources of the two ions were different, and Beibei is located inland, so it can exclude Cl^- and Na^+ with marine sources. The correlation coefficients of K^+ and NH_4^+ in $PM_{2.1}$ and $PM_{9.0}$ were significantly correlated ($r > 0.50$), indicating that these two might have the same sources, and it also verified the phenomenon earlier that K^+ and NH_4^+ had a similar seasonal variation trend. F^- had a strong correlation with SO_4^{2-} in $PM_{2.1}$, indicating that F^- in fine particles may have the same origin as SO_4^{2-}.

In general, the correlations between Na^+, NH_4^+, K^+, Cl^-, NO_3^-, SO_4^{2-} and total water-soluble ions (Σ(–) and Σ(+)) were stronger in $PM_{2.1}$, but the correlations between Mg^{2+}, Ca^{2+}, F^- and total water-soluble ions were stronger in $PM_{9.0}$. This verified the previous reports that Na^+, NH_4^+, K^+, Cl^-, NO_3^- and SO_4^{2-} are mainly present in fine particles, and Mg^{2+}, Ca^{2+} and F^- are mainly present in coarse particles.

Principal Component Analysis of Water-Soluble Ions in Aerosols

In order to better explore the main sources of water-soluble ions in aerosols in Beibei District, the principal component analysis (PCA) was used to classify and analyze 9 kinds of water-soluble ions in $PM_{2.1}$ and $PM_{9.0}$ (Satsangi *et al.*, 2013). Factor analysis results are summarized in Table 4.

For $PM_{2.1}$, two major factors contributing to a larger variance contribution were screened, and 62.53% of the water-soluble ion sources were explained. Among factors 1, NH_4^+, NO_3^-, SO_4^{2-}, Cl^- and K^+ played a significant role,

Table 4. The results of factor analysis for water-soluble ions in $PM_{2.1}$ and $PM_{9.0}$.

Ion component	$PM_{2.1}$		$PM_{9.0}$		
	Factor 1	Factor 2	Factor 1	Factor 2	Factor 3
Na^+	0.521	0.097	0.299	–0.069	0.890
NH_4^+	0.925	–0.283	0.852	–0.359	0.007
K^+	0.745	–0.098	0.722	–0.187	–0.350
Mg^{2+}	0.316	0.678	0.365	0.815	0.179
Ca^{2+}	0.298	0.739	0.554	0.531	–0.189
F^-	0.389	0.515	0.769	0.114	–0.233
Cl^-	0.789	–0.189	0.760	0.276	0.070
NO_3^-	0.892	–0.257	0.892	–0.268	–0.020
SO_4^{2-}	0.846	0.033	0.829	–0.227	0.197
Variance contribution rate (%)	46.161	16.365	49.233	14.762	12.016
Cumulative variance contribution rate (%)	46.161	62.526	49.233	63.995	76.011

and their load coefficients were more than 0.70. SNA mainly came from the secondary transformation of gaseous precursors; Cl^- and K^+ were mainly derived from combustion processes, indicating that factors 1 mainly refer to the secondary transformation process of anthropogenic pollutants and combustion sources. The effects of Ca^{2+}, Mg^{2+} and F^- were significant in factors 2, and their load coefficients reached more than 0.50. Ca^{2+} is the identifying element of building materials, and Ca^{2+} and Mg^{2+} in aerosol mainly come from building, road dust and soil particles. Therefore, factors 2 mainly refer to dust and soil sources.

For $PM_{9.0}$, three main factors contributing to a larger variance contribution were screened, explaining 76.01% of the source of water-soluble ions. Among the factors 1, SNA played a significant role, and their load coefficients were more than 0.80, indicating that factors 1 mainly refer to the secondary transformation process of anthropogenic pollution sources. In factors 2, the effects of Ca^{2+} and Mg^{2+} were significant, and the results were similar to the analysis result of factors 2 for $PM_{2.1}$. In factors 3, only Na^+ had a very significant effect, and its load coefficient was up to 0.89. Part of Na^+ came from marine sources, coexisting with Cl^-, and the other part was mainly related to soil and dust. Beibei District in Chongqing is located inland, so Na^+ was mainly derived from soil. Therefore, factors 3 may be soil sources, and factors 2 may be the dust from building construction and road construction.

The results of principal component analysis showed that the contribution rate of factors 1 in $PM_{2.1}$ and $PM_{9.0}$ was much higher than that of other factors, which indicates that water-soluble ions in aerosol from Beibei mainly come from vehicle exhaust emissions, fossil fuel and biomass fuel combustion. And the maximum load factor in factors 1 was SNA, showing that the secondary ions produced by NH_3 (anthropogenic and natural sources), NO_x and SO_2 (emitted from fuel combustion) under certain meteorological conditions are the most important sources of water-soluble ions. Furthermore, the dust from soil and road construction also contributed to the production of water-soluble ions.

Formation Mechanism of Sulfate and Nitrate in Different Particle Sizes

To investigate the extent to which SO_2 was converted to SO_4^{2-} and NO_2 was converted to NO_3^-, sulfur oxidation ratios (SOR) and nitrogen oxidation ratios (NOR) were calculated, which can clearly indicate secondary transformation processes (Behera and Sharma, 2010). These two conversion ratios are defined as follows (Cheng *et al.*, 2011):

$$SOR = \frac{\left[SO_4^{2-}\right]}{\left[SO_4^{2-}\right]+\left[SO_2\right]} \tag{3}$$

$$NOR = \frac{\left[NO_3^-\right]}{\left[NO_3^-\right]+\left[NO_2\right]} \tag{4}$$

Size distributions of the apparent conversion rate (SOR and NOR) in each season are plotted in Fig. 6. Many studies have found that higher SOR and NOR values imply that the photochemical oxidation of precursor gases has led to the formation of larger proportions of sulfate- and nitrate-containing secondary aerosol particles (Wang *et al.*, 2005b; Sun *et al.*, 2006). Ohta *et al.* (1990) identified it would occur the transformation from SO_2 in the atmosphere when SOR > 0.10. As shown in Fig. 6, SOR values over the four seasons were greater than 0.10 in the fine particles and lower than 0.10 in the coarse particles, which indicated the conversion of SO_2 mostly occurs in the fine particles. SOR was the highest in summer and lowest in winter, implying stronger photochemical reactions of SO_2 in summer. Meanwhile, it could be more conducive to the secondary conversion of SO_2 with a higher temperature, relative humidity and O_3 concentration. More remarkably, the SOR value of the condensation-mode (0.43–0.65 μm) was greater than 0.10 in summer, unlike that in the other seasons. It explained that SO_4^{2-} was mainly from the oxidation of SO_2 with subsequent hygroscopic growth, corresponding with the previous discussion (3.2.2). SOR values were slightly larger than 0.10 in spring and autumn in the ranges of 0.65–1.10 μm and 0.65–2.10, respectively, implying that photochemical oxidation of SO_2 was not the main process. SOR values were all less than 0.10 for each particle size in winter, while SO_4^{2-} concentration was the highest, secondary conversion efficiency of SO_2 in winter was much lower

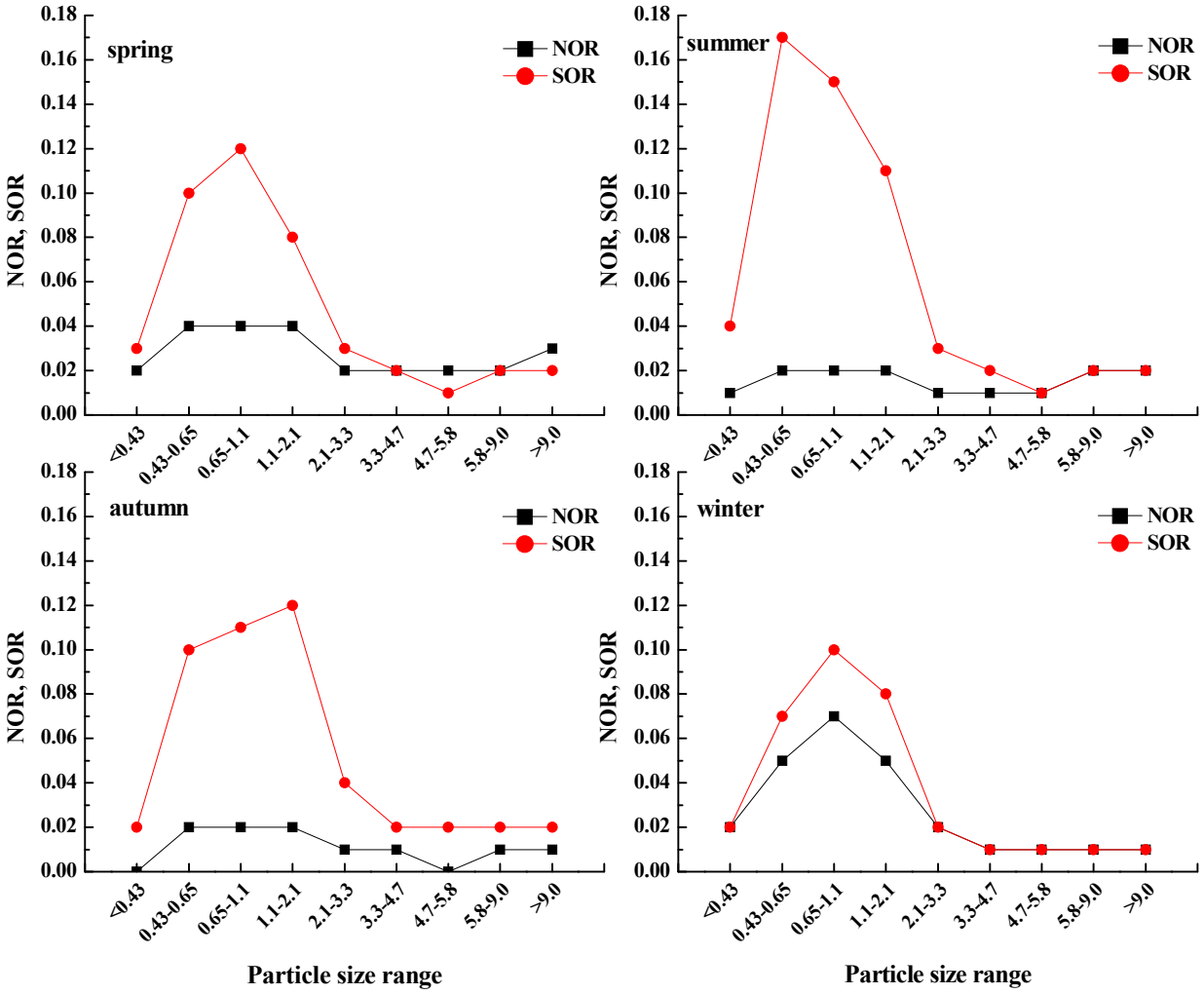

Fig. 6. Size distributions of apparent conversion rate (SOR and NOR) in each season.

than other seasons. Higher SO_4^{2-} accompanied lower SOR, indicating that the sources might mainly come from the long-range transportation, leading to the heterogeneous reaction of SO_2 (Wu *et al.*, 2017).

As shown in Fig. 6, NOR values of the fine-mode over the four seasons were greater than those of the coarse-mode, indicating that the conversion of NO_2 mostly occurred in the fine particles. NOR values were lower than 0.10 in all particles, implying that the oxidation ratios of nitrogen existed at a very low level. NOR values in winter were significantly higher than in other seasons and had great correlation with SOR in the fine particles. NOR in summer was the lowest, probably due to temperature. The volatile NH_4NO_3 can be decomposed into NH_3 and HNO_3 at high temperatures, which might lead to the lower NOR (Suzuki *et al.*, 2008). Furthermore, high temperatures and high photochemical reactions in summer are not only conducive to the conversion of the particulate state to the gaseous state, such as NH_4NO_3, but also conducive to HNO_3 to NO_2 conversion, resulting in decreased NO_3^- and increased NO_2.

In this study, SOR was obviously higher than NOR at the same particle size during the whole year, indicating that the degree of oxidation of sulfate is greater than of nitrogen nitrate in aerosol from 2004 March till 2015 February in Beibei District. The NOR is considerably lower than the SOR, indicating that the SOR and NOR could be the result of different ways in which sulfate- and nitrate-rich particles form and of differences in their sources and removal (Zhang *et al.*, 2011).

CONCLUSION

(1) Due to different levels of meteorological factors in Chongqing during the four seasons, some differences in the size characteristics and the formation mechanisms of these ions were found. SO_4^{2-} was mainly distributed in the droplet mode in spring and autumn, and the formation was attributed to in-cloud processes. In summer, SO_4^{2-} was distributed in the condensation mode and the droplet mode, with a peak in the range of 0.43–0.65 μm, mainly from the oxidation of SO_2 with subsequent hygroscopic growth. Except during summer, the correlation between NH_4^+ and NO_3^- was significant, and mainly existed in the range of 0.65–1.10 μm in the droplet and in the form of NH_4NO_3 in aerosol. In summer, NO_3^- showed a double

distribution and mainly existed in the form of $Ca(NO_3)_2$ in the coarse mode. Na^+ exhibited a single-peak type distribution in spring and summer but appeared as a double peak type in autumn and winter. K^+ showed a single peak type in each season and mainly appeared in the fine mode. The existent forms of Cl^- were KCl in the fine mode and $CaCl_2$ in the coarse mode. Mg^{2+}, Ca^{2+} and F^- were mainly present in the coarse particles during the whole year. Mg^{2+} showed a bimodal pattern distribution in spring and summer and less distribution in autumn and winter. The concentration of Ca^{2+} increased with particle size.

(2) A certain correlation existed between different ions in $PM_{2.1}$ and $PM_{9.0}$, and the concentrations of cations were significantly higher than those of anions. The correlations between Na^+, NH_4^+, K^+, Cl^-, NO_3^-, SO_4^{2-} and the total water-soluble ions were stronger in $PM_{2.1}$, but the correlations between Mg^{2+}, Ca^{2+}, F^- and the total water-soluble ions were stronger in $PM_{9.0}$.

(3) The emissions from motor vehicle exhaust, combustion processes, soil and building construction dust were the major sources of water-soluble ions in Beibei District.

(4) The conversion of SO_2 and NO_2 mainly occurred in the fine particles. SOR was highest in summer and lowest in winter, but NOR in winter was highest compared to the other seasons. The SOR value of the condensation-mode (0.43–0.65 μm) was greater than 0.10 only in the summer, indicating that SO_4^{2-} in summer was mainly from the oxidation of SO_2 with subsequent hygroscopic growth. Higher SO_4^{2-} accompanied lower SOR in winter, indicating that the sources might come primarily from long-range transportation, resulting in the heterogeneous reaction of SO_2. NOR in summer was the lowest, probably due to temperature and photochemical reaction. SOR was considerably higher than NOR at the same particle size during the whole year, indicating a higher degree of oxidation for sulfate than nitrate in aerosol from March 2004 till February 2015 in Beibei District.

ACKNOWLEDGEMENTS

This study was jointly supported by the Key Program of National Natural Science Foundation of China (41230642), the National Natural Science Foundation of China (41275160), the Strategic Pilot Science and Technology Project of the Chinese Academy of Sciences (XDA05100100) and the Fundamental Research Funds for the Central Universities (XDJK2015A013).

REFERENCES

Begam, G.R., Vachaspati, C.V., Ahammed, Y.N., Kumar, K.R., Reddy, R.R., Sharma, S.K., Saxena, M. and Mandal, T.K. (2017). Seasonal characteristics of water-soluble inorganic ions and carbonaceous aerosols in total suspended particulate matter at a rural semi-arid site, Kadapa (India). *Environ. Sci. Pollut. Res.* 24: 1719–1734.

Behera, S.N. and Sharma, M. (2010). Investigating the potential role of ammonia in ion chemistry of fine particulate matter formation for an urban environment. *Sci. Total. Environ*. 408: 3569–3575.

Cao, S., Dan, W., Chen, L.Z., Xia, J.R., Lu, J.G., Liu, G., Li, F.Y. and Yang, M. (2016). Characteristics of water-soluble inorganic ions of aerosol in China. *Environ. Sci. Technol.* 39: 103–115.

Chen, H.H., Dui, W.U., Tan, H.B., Fei, L.I. and Fan, S.J. (2010). Study on the character of haze weather process from the year 2001 to 2008 over the Pearl River Delta. *J. Trop. Meteorol*. 26: 147–155.

Chen, J., Qiu, S.S., Shang, J., Wilfrid, O.M.F., Liu, X.G., Tian, H.Z. and Boman, J. (2014). Impact of relative humidity and water soluble constituents of $PM_{2.5}$ on visibility impairment in Beijing, China. *Aerosol Air Qual. Res.* 14: 260–268.

Chen, L.W., Chow, J.C., Doddridge, B.G., Dickerson, R.R., Ryan, W.F. and Mueller, P.K. (2003). Analysis of a summertime $PM_{2.5}$ and haze episode in the Mid-Atlantic region. *J. Air Waste Manage. Assoc.* 53: 946–956.

Chen, W.H., Wang, X.M., Cohen, J.B., Zhou, S.Z., Zhang, Z.S., Chang, M. and Chan, C.Y. (2016). Properties of aerosols and formation mechanisms over southern China during the monsoon season. *Atmos. Chem. Phys*. 16: 13271–13289.

Chueinta, W., Hopke, P.K. and Paatero, P. (2000). Investigation of sources of atmospheric aerosol at urban and suburban residential areas in Thailand by positive matrix factorization. *Atmos. Environ*. 34: 3319–3329.

Dlugi, R., Jordan, S. and Lindemann, E. (1981). The heterogeneous formation of sulfate aerosols in the atmosphere. *J. Aerosol. Sci.* 12: 185–197.

He, K., Zhao, Q., Ma, Y., Duan, F., Yang, F., Shi, Z. and Chen, G. (2012). Spatial and seasonal variability of $PM_{2.5}$ acidity at two Chinese megacities: Insights into the formation of secondary inorganic aerosols. *Atmos. Chem. Phys.* 12: 1377–1395.

He, Q., Yan, Y., Guo, L., Zhang, Y., Zhang, G. and Wang, X. (2017). Characterization and source analysis of water-soluble inorganic ionic species in $PM_{2.5}$ in Taiyuan city, China. *Atmos. Environ*. 184: 48–55.

Henning, S., Weingartner, E., Schwikowski, M., Gäggeler, H. W., Gehrig, R., Hinz, K.P., Trimborn, A., Spengler, B. and Baltensperger, U. (2003). Seasonal variation of water-soluble ions of the aerosol at the high-alpine site jungfraujoch (3580 m asl). *J. Geophys. Res.* 108: ACH 8-1–ACH 8-10.

Imhof, D., Weingartner, E., Prév t, A.S.H., Ordó ez, C., Kurtenbach, R., Wiesen, P., Rodler, J., Sturm, P., McCrae, I., Ekström, M. and Baltensperger, U. (2006). Aerosol and NO_x emission factors and submicron particle number size distributions in two road tunnels with different traffic regimes. *Atmos. Chem. Phys.* 6: 2215–2230.

Jiang, C.T., Zhang, D. and Zheng, J.J. (2009). Water soluble ions of PM_{10} in Chongqing. *Environ. Sci. Technol.* 32: 109–112. (in Chinese with English abstract)

John, W., Wall, S.M., Ondo, J.L. and Winklmayr, W. (1990). Modes in the size distributions of atmospheric

inorganic aerosol. *Atmos. Environ*. 24: 2349–2359.

Kerminen, V., Anttila, T., Lehtinen, K. and Kulmala, M. (2011). Parameterization for atmospheric new-particle formation: Application to a system involving sulfuric acid and condensable water-soluble organic vapors. *Aerosol Sci. Technol.* 38: 1001–1008.

Li, X.R., Wang, L.L., Ji, D.S., Wen, T.X., Pan, Y.P., Sun, Y. and Wang, Y.S. (2013). Characterization of the size-segregated water-soluble inorganic ions in the Jing-Jin-Ji urban agglomeration: Spatial/temporal variability, size distribution and sources. *Atmos. Environ*. 77: 250–259.

Li, Z.Y., Liu, Y.S., Lin, Y.J., Gautam, S.H., Kuo, H.C., Tsai, C.J., Yeh, H.J., Huang, W., Li, S.W. and Wu, G.J. (2017). Development of an automated system (PPWD/PILS) for studying $PM_{2.5}$ water-soluble ions and precursor gases: Field measurements in two cities, Taiwan. *Aerosol Air Qual. Res.* 17: 426–443.

Liu, Z., Xie, Y.Z., Hu, B., Wen, T.X., Xin, J.Y., Li, X.R. and Wang, Y.S. (2017). Size-resolved aerosol water-soluble ions during the summer and winter seasons in Beijing: Formation mechanisms of secondary inorganic aerosols. *Chemosphere* 183: 119–131.

Meng, Z. and Seinfeld, J.H. (1994). On the source of the submicrometer droplet mode of urban and regional aerosols. *Aerosol Sci. Technol.* 20: 253–265.

Ohta, S. and Okita, T. (1990). A chemical characterization of atmospheric aerosol in Sapporo. *Atmos. Environ*. 24: 815–822.

Pakkanen, T.A., Kerminen, V.M., Hillamo, R.E., Makinen, M., Makela, T. and Virkkula, A. (1996). Distribution of nitrate over sea-salt and soil derived particles—implications from a field study. *J. Atmos. Chem.* 24: 189–205.

Parmar, R.S., Satsangi, G.S., Kumari, M., Lakhani, A., Srivastava, S.S. and Prakash, S. (2001). Study of size distribution of atmospheric aerosol at Agra. *Atmos. Environ*. 35: 693–702.

Satsangi, A., Pachauri, T., Singla, V., Lakhani, A. and Kumari, K.M. (2013). Water soluble ionic species in atmospheric aerosols: Concentrations and sources at Agra in the Indo-Gangetic Plain (IGP). *Aerosol Air Qual. Res.* 13: 1877–1889.

Seinfeld, J.H. and Pandis, S.N. (2006). *Atmospheric chemistry and physics: From air pollution to climate change*, second ed. John Willey & Sons, Inc., New York.

Shen, Z.X., Zhang, L.M., Cao, J.J., Tian, J., Liu, L., Wang, G.H., Zhao, Z.Z., Wang, X., Zhang, R.J. and Liu, S.X. (2012). Chemical composition, sources, and deposition fluxes of water-soluble inorganic ions obtained from precipitation chemistry measurements collected at an urban site in northwest China. *J. Environ. Monit.* 14: 3000–3008.

Sorooshian, A., Shingler, T., Harpold, A., Feagles, C.W., Meixner, T. and Brooks, PD. (2013). Aerosol and precipitation chemistry in the Southwestern United States: spatiotemporal trends and interrelationships. *Atmos. Chem. Phys.* 13: 8615–8662.

Su, J., Zhao, P.S. and Dong, Q. (2018). Chemical compositions and liquid water content of size-resolved aerosol in Beijing. *Aerosol Air Qual. Res.* 18: 680–692.

Sun, Y.L., Zhuang, G.S., Tang, A.H. Wang, Y. and An, Z. (2006). Chemical characteristics of $PM_{2.5}$ and PM_{10} in haze–fog episodes in Beijing. *Environ. Sci. Pollut. Res.*. 40: 3148–3155.

Suzuki, I., Hayashi, K., Igarashi, Y., Takahashi, H., Sawa, Y., Ogura, N., Akagi, T. and Dokiya, Y. (2008). Seasonal variation of water-soluble ion species in the atmospheric aerosols at the summit of Mt. Fuji. *Atmos. Environ.* 42: 8027–8035.

Szopa, S., Balkanski, Y., Schulz, M., Bekki, S., Cugnet, D., Fortems-Cheiney, A., Turquety, S., Cozic, A., Déandreis, C. and Hauglustaine, D. (2013). Aerosol and ozone changes as forcing for climate evolution between 1850 and 2100. *Clim. Dynam*. 40: 2223–2250.

Tang, A.H., Zhuang, G.S., Wang, Y., Yuan, H. and Sun, Y.L. (2005). The chemistry of precipitation and its relation to aerosol in Beijing. *Atmos. Environ*. 39: 3397–3406.

Tao, Y., Yin, Z., Ye, X.N., Ma, Z. and Chen, J.M. (2014). Size distribution of water-soluble inorganic ions in urban aerosols in Shanghai. *Atmos. Pollut. Res.* 5: 639–647.

Tian, M., Wang, H.B., Chen, Y., Zhang, L.M., Shi, G.M., Liu, Y., Yu, J.Y., Zhai, C.Z., Wang, J. and Yang, F.M. (2016a). Highly time-resolved characterization of water-soluble inorganic ions in $PM_{2.5}$ in a humid and acidic mega city in Sichuan Basin, China. *Sci. Total Environ.* 580: 224–234.

Tian, S.L., Pan, Y.P. and Wang, Y.S. (2016b). Size-resolved source apportionment of particulate matter in urban Beijing during haze and non-haze episodes. *Atmos. Chem. Phys.* 16: 1–19.

Wan, X., Kang, S.C., Xin, J.J., Liu, B., Wen, T.X., Wang, P.L., Wang, Y.S. and Cong, Z.Y. (2016). Chemical composition of size-segregated aerosols in Lhasa city, Tibetan Plateau. *Atmos. Res.* 174–175: 142–150.

Wang, H. and Shooter, D. (2001). Water soluble ions of atmospheric aerosols in three New Zealand cities: Seasonal changes and sources. *Atmos. Environ*. 35: 6031–6040.

Wang, H., Zhu, B., Shen, L., Xu, H., An, J., Xue, G. and Cao, J. (2015). Water-soluble ions in atmospheric aerosols measured in five sites in the Yangtze River Delta, China: Size-fractionated, seasonal variations and sources. *Atmos. Environ*. 123: 370–379.

Wang, L., Ji, D.S., Li, Y., Gao, M., Tian, S.L., Wen, T.X., Liu, Z.R., Wang, L.L., Xu, P., Jiang, C.S. and Wang, Y.S. (2017). The impact of relative humidity on the size distribution and chemical processes of major water-soluble inorganic ions in the megacity of Chongqing, China. *Atmos. Res.* 192: 19–29.

Wang, Y., Zhuang, G.S., Sun, Y.L. and An, Z. (2005a). Water-soluble part of the aerosol in the dust storm season-evidence of the mixing between mineral and pollution aerosol. *Atmos. Environ*. 39: 7020–7029.

Wang, Y., Zhuang, G. and Tang, A. (2005b). The ion chemistry and the source of $PM_{2.5}$ aerosol in Beijing. *Atmos. Environ*. 39: 3771–3784.

Wu, X., Deng, J.J., Chen, J.S., Hong, Y.W., Xu, L.L., Yin, L.Q., Du, W.J., Hong, Z.Y., Dai, N.Z. and Yuan, C.S.

(2017). Characteristics of water-soluble inorganic components and acidity of $PM_{2.5}$ in a coastal city of China. *Aerosol Air Qual. Res.* 17: 2152–2164.

Xu, L., Chen, X., Chen, J., Zhang, F., He, C., Zhao, J. and Yin, L. (2012). Seasonal variations and chemical compositions of $PM_{2.5}$ aerosol in the urban area of Fuzhou, China. *Atmos. Res*. 104–105: 264–272.

Yang, C., Peng, X., Huang, W., Chen, R., Xu, Z., Chen, B. and Kan, H. (2012). A time-stratified case-crossover study of fine particulate matter air pollution and mortality in Guangzhou, China. *Int. Arch. Occup. Environ. Health* 85: 579.

Yang, Y.Y., Zhou, R., Wu, J.J., Yu, Y., Ma, Z.Q., Zhang, L.J. and Di, Y.A. (2015). Seasonal variations and size distributions of water-soluble ions in atmospheric aerosols in Beijing, 2012. *J. Environ. Sci.* 34: 197–205.

Yue, D.L., Zhong, L.L., Zhang, T., Shen, J., Yuan, L., Ye, S.Q., Zhou, Y. and Zeng, L.M. (2016). Particle growth and variation of cloud condensation nucleus activity on polluted days with new particle formation: A case study for regional air pollution in the PRD region, China. *Aerosol Air Qual. Res.* 16: 323–335.

Zhang, T., Cao, J.J., Tie, X.X., Shen, Z.X., Liu, S.X., Ding, H., Han, Y.M., Wang, G.H., Ho, K.F. and Qiang, J. (2011). Water-soluble ions in atmospheric aerosols measured in Xi'an, China: Seasonal variations and sources. *Atmos. Res.* 102: 110–119.

Zhou, Y., Fu, J.S., Zhuang, G. and Levy, J.I. (2010). Risk-based prioritization among air pollution control strategies in the Yangtze River Delta, China. *Environ. Health Perspect.* 118: 1204–1210.

Zhuang, H, Chan, C.K., Fang, M. and Wexler, A.S. (1999). Formation of nitrate and non-sea-salt sulfate on coarse particles. *Atmos. Environ*. 33: 4223–4233.

Received for review, December 10, 2017
Revised, January 29, 2018
Accepted, January 30, 2018